

Physico-chemical characterization and dissolution properties of nifluminic acid-cyclodextrin-PVP ternary systems

R. Ambrus · Z. Aigner · L. Catenacci ·
G. Bettinetti · P. Szabó-Révész · M. Sorrenti

Received: 8 July 2010/Accepted: 16 September 2010/Published online: 12 October 2010
© Akadémiai Kiadó, Budapest, Hungary 2010

Abstract In view of the poor aqueous solubility of nifluminic acid (NIF), the aim of this article was to improve its solubility and dissolution rate through the preparation of formulations based on hydroxypropyl β -cyclodextrin (HP β CD) and polyvinylpyrrolidone K25 (PVP K25), a combination of carriers which has been advantageously used for a similar purpose with various hydrophobic drugs. Ternary systems of NIF, HP β CD, and PVP K25 were prepared in different drug to CD to PVP ratios by physical mixing, kneading, microwave irradiation, and co-evaporation. Differential scanning calorimetry, thermogravimetric analysis, hot stage microscopy, Fourier transform infrared spectroscopy, and X-ray powder diffractometry were used to investigate the resulting solid-state interactions. The results showed that the solid state of the drug in the amorphous or crystalline ternary combinations influenced both the solubility and the dissolution rate of NIF.

Keywords Dissolution · FT-IR · Nifluminic acid · Thermal analysis · X-ray powder diffraction

Introduction

The aqueous solubility and the dissolution rate of the drug from oral solid dosage forms have a relevant impact on the bioavailability of the active ingredient. Nifluminic acid

(NIF), a structural analog of anthranilic acid, has anti-inflammatory activity accompanied by an analgesic effect; it is primarily used to treat different forms of rheumatism, e.g., rheumatoid arthritis and arthrosis, and other inflammatory states [1, 2]. According to the Biopharmaceutics Classification System (BCS), NIF belongs to class II, a practically water-insoluble ($26 \mu\text{g mL}^{-1}$ at 25°C), lipophilic, and highly permeable compound [3]. Since NIF is widely prescribed for mild illnesses, the safety aspect becomes central, and optimization of the overall drug pharmacological profile is an important objective [4].

Among the various methods used to improve the solubility/dissolution rate of poorly water soluble drugs, the preparation of solid dispersions [5–8] or of inclusion complexes of drug with cyclodextrins (CDs) [9–11] are the most frequently employed. In fast-release solid dispersions, a hydrophilic polymer of first choice is polyvinylpyrrolidone (PVP), which is commercially available with various average molecular weights and marked complexing and solubilizing properties [12–14]. On the other hand, hydroxypropyl β -CD (HP β CD) is one of the pharmaceutically acceptable carrier due to its amorphousness, high water solubility, high solubilizing ability, low cost, and low toxicity [15–18]. In a previous article, the system of NIF with HP β CD was investigated to improve the dissolution properties of the drug [19]. The results revealed that an increase of the CD content in the product corresponded to an increased NIF dissolution rate; in particular, at a NIF-CD 1:1 mol ratio, the increase was 1.54-fold.

The favorable effects of PVP on the solubility and on the dissolution rate of anti-inflammatory non-steroidal drugs are well documented [18, 20–23], as well as the positive effect of the addition of small amounts of PVP on the complexation of CD in terms of the increase in apparent stability constant and drug availability [24–29].

R. Ambrus · Z. Aigner · P. Szabó-Révész
Department of Pharmaceutical Technology, University
of Szeged, 6720 Eötvös u. 6, Szeged, Hungary

L. Catenacci · G. Bettinetti · M. Sorrenti (✉)
Department of Pharmaceutical Chemistry, University of Pavia,
Via Taramelli 12, 27100 Pavia, Italy
e-mail: milena.sorrenti@unipv.it

The objective of this study was to characterize the ternary combinations of NIF with HP β CD and PVP. The ternary systems, in different drug to CD to PVP ratios, were prepared by using different methods such as simple physical mixing, kneading, co-evaporation, and microwave irradiation [30], as described in the experimental section. Differential scanning calorimetry (DSC), thermogravimetric analysis (TG), and hot stage microscopy (HSM), supported by Fourier transform infrared spectroscopy (FT-IR) and X-ray powder diffractometry (XRPD), were used to investigate the solid-state interactions between NIF, HP β CD, and PVP. In vitro aqueous solubility and dissolution rate profiles of the ternary systems were also performed.

Experimental

Materials

NIF, chemically 2-[[3-(trifluoromethyl)phenyl]amino]-3-pyridinecarboxylic acid, from G. Richter Pharmaceutical Factory, Hungary; HP β CD from Cyclolab R&D Laboratory Ltd., Budapest, Hungary; and PVP K25 ($M_w \sim 34000$) from ISP Customer Service GmbH, Germany were used. All the other materials and reagents were of analytical grade purity.

Sample preparation

The compositions of the ternary systems prepared are listed in Table 1. The CD:NIF ratios are given on molar basis, and the NIF:PVP ratios on a mass basis.

Physical mixtures (PMs) were prepared by gently grinding of the powder components together in a mortar with a pestle and passing through a 100- μ m sieve.

Table 1 Compositions of ternary systems prepared by physical mixing (PM), kneading (KP), co-evaporation (CP), and microwave irradiation (MP)

NIF:HP β CD:PVP*	PM	KP	CP	MP
9:1:1	X	–	–	–
6:1:1	X	–	–	–
3:1:1	X	–	–	–
2:1:1	X	–	–	–
1:1:1	X	X	X	X
1:2:1	X	X	X	X
1:3:1	X	X	X	X
1:1:2	–	X	X	–
1:2:2	–	X	X	–
1:3:2	X	X	X	X

* NIF:CD on molar ratio, NIF:PVP on mass ratio

Kneaded products (KPs) were prepared by wetting each PM in a mortar with ethanol:water 1:1 (v/v) and grinding thoroughly with a pestle, after which the product was dried to constant weight at room temperature. The samples were then sieved through a 100- μ m sieve.

Co-evaporated products (CPs) were prepared by dissolving NIF in acetone (1 g in 30 mL), and then adding the appropriate amounts of PVP K25 and HP β CD and then minimum amount of methanol (~10 mL) to obtain a clear solution. The solvents were removed under reduced pressure at 30 °C, and the residue was dried under vacuum at room temperature for 3 h, gently ground in a mortar with a pestle, and passed through a 100- μ m sieve.

Microwave irradiation products (MPs) were prepared by wetting each PM with 33% (w/v) aqueous ethanol solution (200 mg in ~6 mL) in a glass container, followed by homogenization with a pestle for 3 min and microwave irradiation at 425 W for 10 min (Pabish CM-Aquatronic). The dried residue was gently ground in a mortar with a pestle, and passed through a 100- μ m sieve.

All products were stored in a desiccator (P₂O₅) at room temperature (25 °C).

Methods

Temperature and enthalpy values were measured with a Mettler STAR^e system equipped with a DSC 821^e Module on 3–5 mg (Mettler M3 microbalance) samples in sealed aluminum pans with a pierced lid ($\beta = 5 \text{ K min}^{-1}$, static air atmosphere, 30–300 °C temperature range). Measurements were carried out at least in triplicate.

Mass losses were recorded with a Mettler TA 4000 apparatus equipped with a TG 50 cell on 5–7 mg samples in open alumina crucibles ($\beta = 5 \text{ K min}^{-1}$, static air atmosphere, 30–300 °C temperature range). Measurements were carried out at least in triplicate.

Microscopic observation of sample morphology and thermal events on heating was performed under a Reichert (Arnsberg, Germany) polarized light microscope equipped with a Mettler FP82HT/FP80 system ($\beta = 10 \text{ K min}^{-1}$). Images were taken with a MOTICAM 2000 video camera and elaborated with Adobe Photoshop 7.0.

FT-IR (650–4000 cm⁻¹) spectra were recorded on powder samples with a Spectrum One Perkin–Elmer FT-IR spectrophotometer (resolution 4 cm⁻¹) equipped with a MIRacleTM ATR device (Pike Technologies).

XRPD patterns were taken at ambient temperature with a computer-controlled Philips PW 1800/10 apparatus (powdered samples in Al holders; Cu K $\alpha,1 = 1.54060 \text{ \AA}$, Cu K $\alpha,2 = 1.54439 \text{ \AA}$; 2°–40° 2θ scan range; 0.02° 2θ s⁻¹ scan speed; monochromator: graphite crystal).

Dissolution tests were carried out at 37 ± 0.5 °C with the USP method 2 (USP rotating-paddle dissolution

apparatus, type DT, Erweka, Germany) in 100 mL of simulated gastric medium (SGM) ($\text{pH} = 1.1 \pm 0.1$; 94.00 g of 1 N HCl, 0.35 g of NaCl, 0.50 g of glycine in 1000 mL of distilled water) using 50 mg of NIF or product containing 50 mg of NIF. The paddle was rotated at 100 rpm and sampling was performed up to 120 min (sample volume 5.0 mL). After filtration and appropriate dilution, the NIF amount was determined spectrophotometrically ($\lambda_{(\text{SGM})} = 256 \text{ nm}$). Each experiment was performed in triplicate.

The following mathematical models were used to evaluate the results of the dissolution tests.

Langenbucher model:

$$\sqrt[3]{\frac{m_t}{m_0}} = 1 - \frac{t}{T}$$

Modified Langenbucher:

$$\sqrt[3]{1 - \frac{m_t}{m_0}} = \ln t,$$

where m_0 is the mass of drug at time $t = 0$ and m_t , is that at time t , and T is the total time of the dissolution [31, 32].

The kinetics analyses were carried out with an in vitro–in vivo kinetic computer program.

Results and discussion

The DSC profiles (Fig. 1, on the top) indicate the crystalline, anhydrous state of NIF (curve a) ($T_{m,\text{peak}} = 202.6 \pm 0.5^\circ\text{C}$, $\Delta H_m = 131 \pm 2 \text{ J g}^{-1}$), and the amorphous hydrate nature of HP β CD and PVP with loosely bound water (curves b and c). The TG and DTG curves (Fig. 1, on the bottom) confirm the anhydrous state of NIF (curves a,a') and the presence in both HP β CD and PVP of $\sim 5.5\%$ (as mass fraction) of water, which is lost between 30 and 120 $^\circ\text{C}$ (curves b,b' and c,c').

In Fig. 2 are reported DSC curves of PMs containing different ratios of NIF (NIF:PVP 9:1, 6:1, 3:1, 2:1, and 1:1 (w/w), curves a, b, c, d, and e, respectively), maintaining 1 mol of HP β CD in each combinations. As the quantity of NIF in the PMs decreases, the endothermic effect of drug melting is progressively broadened and the enthalpy value lowered, until disappearance at the composition 2:1:1 (see curve d), as a consequence of drug amorphization and/or drug–carrier interaction.

In Fig. 3 the DSC curves at the composition 1:1:1 for the PM, KP, MP, and CP are reported. The melting peak of NIF is absent in the PM and CP products (curves a and d), while is still present in the DSC curves of the KP and MP (curves b and c) as a very small endothermic effect around 172 $^\circ\text{C}$ ($\Delta H_m = 46 \text{ J g}^{-1}$ and $\Delta H_m = 18 \text{ J g}^{-1}$, respectively) probably due to the residual drug crystallinity.

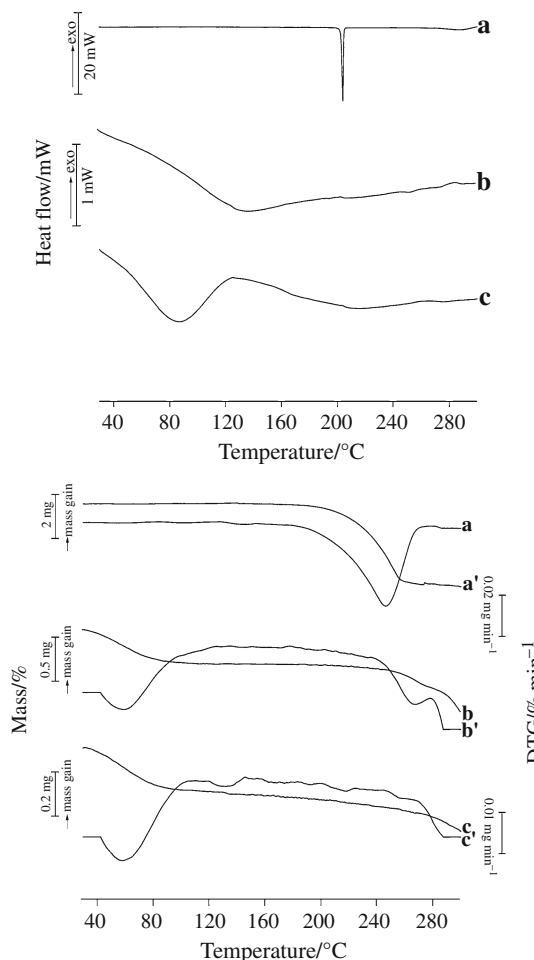


Fig. 1 Top DSC curves of NIF (a), HP β CD (b), and PVP K25 (c); bottom TG and DTG curves of NIF (a,a'), HP β CD (b,b'), and PVP K25 (c,c')

In Fig. 4 are reported XRPD patterns of NIF (pattern a) and the NIF:HP β CD:PVP 1:1:1 physical mixture (pattern b) and the respective co-evaporated product (pattern c). XRPD patterns confirm the crystalline nature of the drug, with characteristic peaks at diffraction angles of 8.18, 12.92, 16.33, 21.30, and 23.21 $^\circ\text{2}\theta$, still evident in the XRPD pattern of PM, despite the flat DSC profile in the temperature region of drug melting (Fig. 3, curve a). Such behavior can be explained assuming NIF amorphization (i.e., dissolution) in the amorphous carrier solution (as solvent), brought about by thermal energy absorbed during the DSC scan. This effect was already described for naproxen [18]. The XRPD pattern of CP product confirms the amorphous nature of this system such as just revealed by the flat DSC curve (Fig. 3, curve d).

All the other samples listed in Table 1 show a thermal behavior very similar to that reported for the 1:1:1 composition, and the DSC and TG curves are, therefore, not reported.

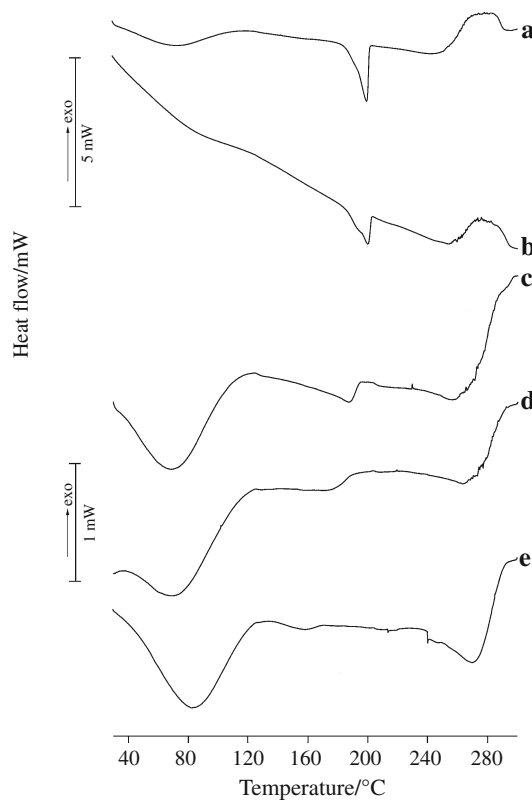


Fig. 2 DSC curves of NIF:HP β CD:PVP K25 PMs at 9:1:1 (*a*), 6:1:1 (*b*), 3:1:1 (*c*), 2:1:1 (*d*), and 1:1:1 (*e*) compositions

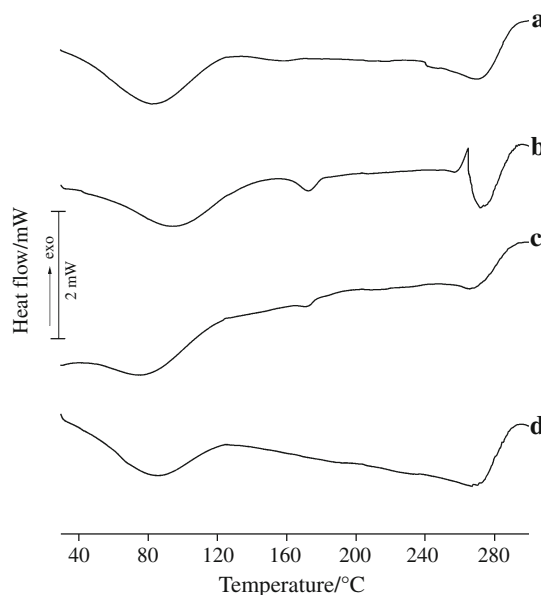


Fig. 3 DSC curves of the NIF:HP β CD:PVP K25 (1:1:1) physical mixture (*a*) and the respective kneading (*b*), microwave-irradiated (*c*), and co-evaporated (*d*) products

In Fig. 5 are reported HSM photomicrographs of the raw NIF (a), the NIF:HP β CD:PVP 1:1:1 physical mixture (b), and the respective co-evaporated product (c), recorded at

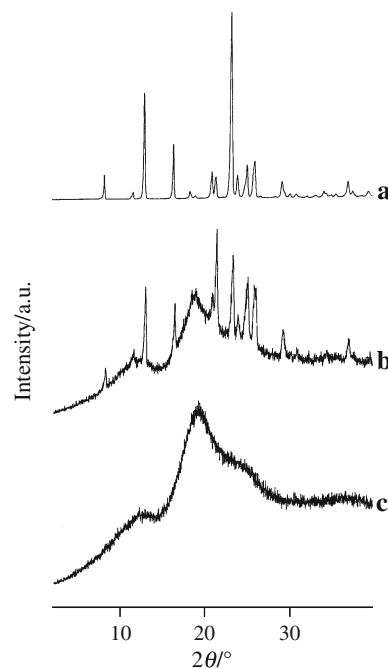


Fig. 4 XRPD patterns of NIF (*a*), the NIF:HP β CD:PVP K25 (1:1:1) physical mixture (*b*), and the respective co-evaporated product (*c*)

the various temperatures indicated in the pictures. Pure NIF crystals appear as plates. When heated under ambient atmosphere from room temperature to ~ 200 °C, the shape of the initial particles is preserved; only a rounded edge is observed just before melting that occurs at 204 °C. At ambient temperature, the presence of some crystals of NIF rounded by amorphous aggregates of the carrier in the PM is evident; the crystal shape is maintained until just before melting at about 156 °C (Fig. 5b). The CP product appears as amorphous sample, and no melting is recorded during heating until decomposition that occurs at 300 °C (Fig. 5c).

In order to further investigate the interaction between the drug and the carrier, FT-IR spectra of each component and all the ternary systems prepared are recorded. The NIF spectrum (Fig. 6a) shows the characteristic absorption bands of the carboxyl group (C=O stretching at 1663 cm^{-1}) and O–H stretching at 1424 cm^{-1} . The CF₃ group signal appears at 1326 cm^{-1} and the characteristic C–H band at around 880 cm^{-1} . The HP β CD spectrum (Fig. 6b) displays the characteristic band of O–H stretching at around 3310 cm^{-1} . In the PVP K25 spectrum (Fig. 6c), a strong band due to the C=O stretching vibration and a broad strong band due to the O–H stretching vibration at 1650 cm^{-1} and at 3440 cm^{-1} , respectively, are present.

The FT-IR spectrum of the PM (Fig. 6d) is very similar to that of HP β CD, probably because in this ratio (1:1:1) the CD is present in higher quantity compared to NIF and PVP. The FT-IR spectra of KP (Fig. 6e) and CP (Fig. 6f)

Fig. 5 HSM photomicrographs of NIF (**a**), the NIF:HP β CD:PVP K25 (1:1:1) physical mixture (**b**), and the co-evaporated product (**c**) recorded at various temperatures

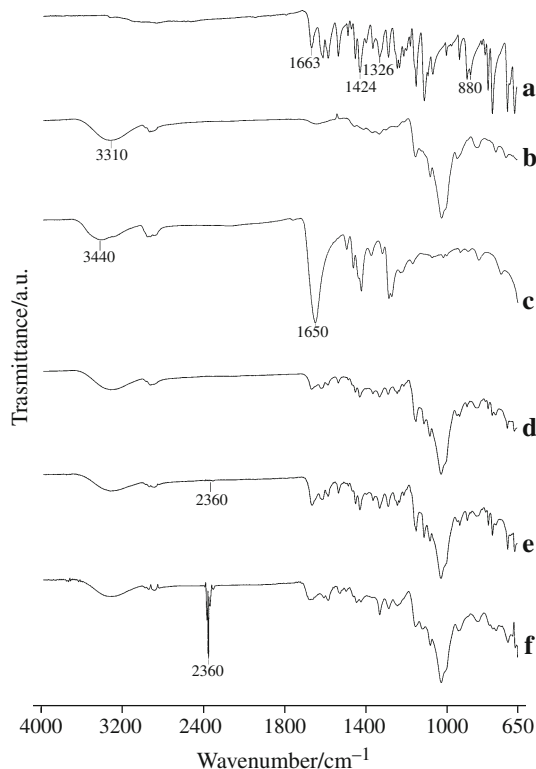
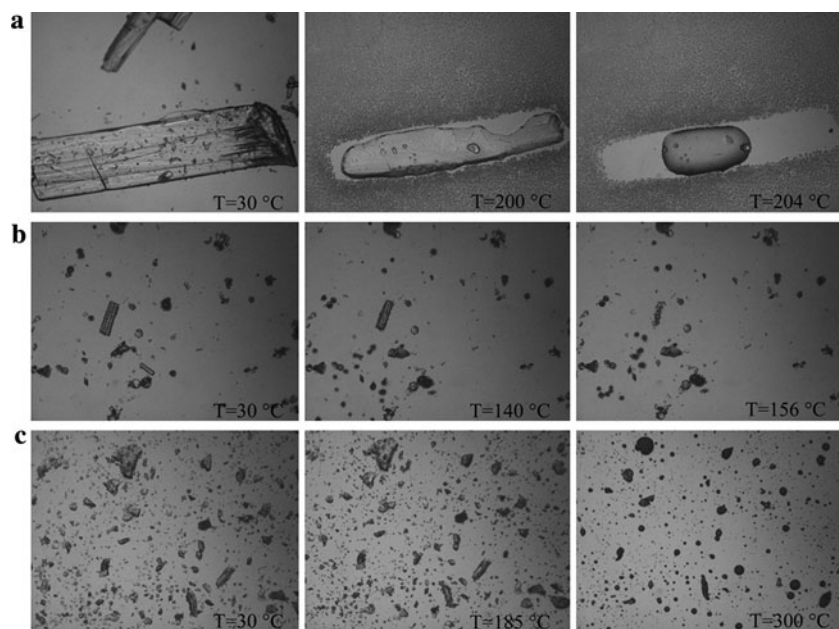


Fig. 6 FT-IR spectra of NIF (**a**), HP β CD (**b**), PVP K25 (**c**), the NIF:HP β CD:PVP K25 (1:1:1) physical mixture (**d**), and the respective kneading (**e**), and co-evaporated (**f**) products

products in the region between 1700 and 1200 cm⁻¹ are very similar; the absorption bands are not well resolved, suggesting an amorphization of the drug. On the other hand, the spectrum of the CP product presents a new band at around 2360 cm⁻¹, due to the $-\text{NH}^{3+}$ stretching

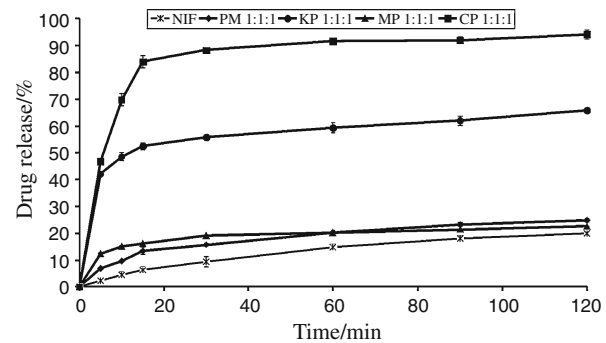


Fig. 7 Dissolution profile of NIF (asterisk), the NIF:HP β CD:PVP K25 (1:1:1) physical mixture (filled diamond), and the respective kneading (filled circle), microwave-irradiated (filled triangle), and co-evaporated (filled square) products

vibration [33]. The crystalline NIF is in the double ion, ammonium-carboxylate state, which is common with the acid. Probably the use of the organic solvent alcohol or acetone induced proton transfer and so the transformation of NIF from the neutral to the amino-carboxylic form.

Niflumic acid is a weak acid ($pK_{a,1} = 2.28 \pm 0.08$, $pK_{a,2} = 4.86 \pm 0.05$ [34]) characterized by very low solubility in aqueous solutions (1.9×10^{-2} mg mL⁻¹ at 25 °C [35]). The in vitro dissolution behavior of pure NIF (50 mg) in SGM is 9.92 mg/100 mL which means that $19.8 \pm 0.4\%$ is released in 120 min (Fig. 7). The processes of dissolution in SGM are prolonged and saturation is observed after 30 min. As concerns the PM and MP products, the quantity of NIF dissolved increases only gradually, an approximately 10% solubility increase being measured, independently of the weight ratios. However, by the kneading (64.0 ± 0.2%) and co-evaporative

Table 2 Kinetic results of NIF and 1:1:1 products

	<i>K</i>	<i>m</i>	<i>R</i> ²
NIF	0.021	-0.031	0.97
PM	0.021	-0.013	0.99
KP	0.038	0.11	0.98
MP	0.012	0.026	0.99
CP	0.12	0.057	0.91

K dissolution rate, *m* intersection, and *R*² correlation coefficient

(94.1 ± 0.3%) technologies, significantly higher dissolution concentration is achieved.

The dissolution of NIF from the products in SGM is described most precisely by the Langenbucher equation. The kinetic of the drug release (dissolution rate constant, *K*) is studied by using the mathematical model presented earlier, as a function of the correlation coefficient of the dissolution process (Table 2). The kinetic parameters are in agreement with the dissolution data and confirm that the drug dissolution depends on the preparation method and that the value of *K* is significantly higher (nearly 6-fold) for the CP product compared to pure NIF.

Conclusions

Thermal characterization of the ternary systems prepared with HP β CD and PVP K25 revealed a solid interaction between the drug and the carrier and/or a drug amorphization, more evident in the systems prepared by physical mixing and co-evaporation. In the kneaded and microwave-irradiated products, only partial drug dispersion in the carrier is demonstrated by the thermal data. The XRPD patterns showed the partially crystalline nature of the physical mixture and the complete drug amorphization in the other systems prepared.

All the ternary systems are suitable to improve the dissolution rate of NIF, a drug with very low aqueous solubility. The dissolution data and the kinetic parameters revealed that the percentage of drug release is dependent on the preparation method used. The best performance is obtained for the CP product, with a dissolution rate constant value nearly sixfold higher than that of pure NIF. However, further studies should be performed concerning the storage and bioavailability of NIF in solid dispersions, because these systems are presumably suitable for the formulation of oral or semisolid dosage forms.

Acknowledgements This study was supported by TÁMOP research project: Development of teranostics in cardiovascular, metabolics, and inflammatory diseases (TÁMOP-4.2.2-08/1-2008-0013).

References

- Insel PA. Analgesic-antipyretics and antiinflammatory agents; drugs employed in the treatment of rheumatoid arthritis and gout. In: Gilman AG, Rall TW, Nies AS, Taylor P, editors. Goodman and Gilman's the pharmacological basis of therapeutics. Singapore: McGraw-Hill; 1991. p. 668.
- Fürst Zs editor. In: Farmakológia. Budapest: Medicina; 2001. p. 845.
- Houin G, Tremblay D, Bree F, Dufour A, Ledugal P, Tillement JP. The pharmacokinetics and availability of niflumic acid in humans. *Int J Clin Pharmacol Ther Toxicol*. 1983;21:130–4.
- Lan SJ, Chando TJ, Weliky I, Schreiber EC. Metabolism of niflumic acid-14C: absorption, excretion and biotransformation by human and dog. *J Pharmacol Exp Ther*. 1973;186:323–30.
- Craig DQM. The mechanisms of drug release from solid dispersions in water soluble polymers. *Int J Pharm*. 2002;231: 131–44.
- Leuner C, Dressman J. Improving drug solubility for oral delivery using solid dispersions. *Eur J Pharm Biopharm*. 2000;50:47–60.
- Chokshia RJ, Sandhu HK, Shah NH, Malick WA. Improving the dissolution rate of poorly water soluble drug by solid dispersion and solid solution-pros and cons. *Drug Deliv*. 2007;14:33–45.
- Patyi G, Bo'dis A, Antal I, Vajna B, Nagy Zs, Marosi Gy. Thermal and spectroscopic analysis of inclusion complex of spironolactone prepared by evaporation and hot melt methods. *J Therm Anal Calorim*. 2010;102:349–55.
- Lutka A. Investigation of interaction of promethazine with cyclodextrins in aqueous solution. *Acta Pol Pharm*. 2002;59: 45–51.
- Zielenkiewicz W, Koźbiel M, Golankiewicz B, Poznański J. Enhancement of aqueous solubility of tricyclic acyclovir derivatives by their complexation with hydroxypropyl- β -cyclodextrin. *J Therm Anal Calorim*. 2010;101:555–60.
- Nisharani SR, Nilesh SK, Parth DM, Arati NR. Improvement of water solubility and in vitro dissolution rate of aceclofenac by complexation with β -cyclodextrin and hydroxypropyl- β -cyclodextrin. *Pharm Dev Technol*. 2010;15:64–70.
- Mashru RC, Sutariya VB, Sankalia MG, Yagnakumar P. Characterization of solid dispersions of rofecoxib using differential scanning calorimeter. *J Therm Anal Calorim*. 2005;82:167–70.
- Tantishaiyakul V, Keawnopparat N, Ingkatawornwong S. Properties of solid dispersions of piroxicam in polyvinylpyrrolidone. *Int J Pharm*. 1999;181:143–51.
- Papageorgiou GZ, Docoslis A, Georgarakis M, Bikiaris D. The effect of physical state on the drug dissolution rate. Miscibility studies of Nimodipine with PVP. *J Therm Anal Calorim*. 2009;95:903–15.
- Taneri F, Güneri T, Aigner Z, Berkesi O, Kata M. Thermoanalytical studies on complexes of ketoconazole with cyclodextrin derivatives. *J Therm Anal Calorim*. 2003;74:769–77.
- Aigner Z, Hassan HB, Berkesi O, Kata M, Erős I. Thermoanalytical, FTIR and X-ray studies of gemfibrozil-cyclodextrin complexes. *J Therm Anal Calorim*. 2005;81:267–72.
- Fröming KH, Szejtli J. Cyclodextrins in pharmacy. Dordrecht: Kluwer Academic Publishers; 1994. p. 74.
- Mura P, Fauci MT, Bettinetti GP. The influence of polyvinylpyrrolidone on naproxen complexation with hydroxypropyl- β -cyclodextrin. *Eur J Pharm Sci*. 2001;13:187–94.
- Kata M, Ambrus R, Aigner Z. Preparation and investigation of inclusion complexes containing niflumic acid and cyclodextrins. *J Incl Phenom*. 2002;44:123–6.
- Valero M, Perez-Revuelta BJ, Rodríguez LJ. Effect of PVP K-25 on the formation of the naproxen-cyclodextrin complex. *Int J Pharm*. 2003;253:97–110.

21. Ambrus R, Aigner Z, Berkesi O, Soica C, Szabó-Révész P. Determination of structural interaction of nifluminic acid-PVP solid dispersions. *Rev Chim.* 2006;57:1051–4.
22. Ambrus R, Aigner Z, Dehelean C, Szabó-Révész P. Physico-chemical studies on solid dispersions of nifluminic acid prepared with PVP. *Rev Chim.* 2007;58:60–4.
23. Ambrus R, Aigner Z, Soica C, Peev C, Szabó-Révész P. Amorphisation of nifluminic acid with polyvinylpyrrolidone prepared solid dispersion to reach rapid drug release. *Rev Chim.* 2007;58:206–9.
24. Loftsson T, Frithriksdóttir H. The effect of water-soluble polymers on the aqueous solubility and complexing abilities of β -cyclodextrin. *Int J Pharm.* 1998;163:115–21.
25. Loftsson T, Masson M, Sigurjonsdóttir JF. Methods to enhance the complexation efficiency of cyclodextrins. *STP Pharma Sci.* 1999;9:237–42.
26. Esclusa-Díaz MT, Gayo-Otero M, Pérez-Marcos MB, Vila-Jato JL, Torres-Labandeira JJ. Preparation and evaluation of ketoconazole- β -cyclodextrin multicomponent complexes. *Int J Pharm.* 1996;142:183–7.
27. Szente L, Szejtli J. Solution for insolubility problems of base-type drugs: multicomponent cyclodextrin complexation. In: Proceedings of 1st world meeting APGI/APV. Budapest; 1995.
28. Granero G, Bertorello MM, Longhi M. Solubilization of a naphthoquinone derivative by hydroxypropyl-beta-cyclodextrin (HP-beta-CD) and polyvinylpyrrolidone (PVP-K30). The influence of PVP-K30 and pH on solubilizing effect of HP-beta-CD. *Boll Chim Farm.* 2002;141:63–6.
29. Patel AR, Vavia PR. Effect of hydrophilic polymers on solubilization of fenofibrate by cyclodextrin complexation. *J Incl Phenom.* 2006;56:247–51.
30. Patil JS, Kadam DV, Marapur SC, Kamalapur MV. Inclusion complex system; a novel technique to improve the solubility and bioavailability of poorly soluble drugs: a review. *Int J Pharm Sci Rev Res.* 2010;2(2):29–34.
31. Salomon JL, Doelker E. Formulation des comprimés à libération prolongée, I. Matrices inertes. *Pharm Acta Helv.* 1980;55:174–82.
32. Langenbucher F. Linearization of dissolution rate curves by the Weibull distribution. *J Pharm Pharmacol.* 1972;24:979–89.
33. Socrates G. Infrared characteristic group frequencies—tables and charts. 2nd ed. Chichester: Wiley; 1994. p. 80.
34. Allen RI, Box KJ, Comer JEA, Peake C, Tam Y. Multiwavelength spectrophotometric determination of acid dissociation constants of ionizable drugs. *J Pharm Biomed Anal.* 1998;17:699–712.
35. Dannenfelser RM, Yalkowsky SH. Database for aqueous solubility of nonelectrolytes. *Comput Appl Biosci.* 1989;5:235–6.